ELSEVIER

Thermochimica Acta 371 (2001) 87–93

thermochimica acta

www.elsevier.com/locate/tca

Characterization of thermoplastic interpenetrating polymer networks by various thermal analysis techniques

A.S. Vatalis[a], C.G. Delides[a], G. Georgoussis[b], A. Kyritsis[b], O.P. Grigorieva[c], L.M. Sergeeva[c], A.A. Brovko[c], O.N. Zimich[c], V.I. Shtompel[c], E. Neagu[d], P. Pissis[b,*]

[a]*Laboratories of Physics and Materials Technology, Technological Education Institute (TEI) of Kozani, 50100 Kila, Kozani, Greece*
[b]*Department of Physics, National Technical University of Athens, Zografou Campus, 15780 Athens, Greece*
[c]*Academy of Sciences of Ukraine, Institute of Macromolecular Chemistry, 253160 Kiev, Ukraine*
[d]*Department of Physics, Technical University of Iasi, 6600 Iasi, Romania*

Received 25 August 2000; accepted 12 December 2000

Abstract

Thermoplastic interpenetrating polymer networks (t-IPNs), prepared by melting and pressing of crystallizable polyurethane (CPU) and styrene/acrylic acid random copolymer (S/AA) in wide ranges of composition, were investigated by the combination of various thermal analysis techniques: differential scanning calorimetry (DSC), thermomechanical analysis (TMA), thermally stimulated depolarization currents (TSDC) and thermally stimulated conductivity (TSC) measurements, as well as broadband dielectric relaxation spectroscopy (DRS). The results show that the t-IPNs under investigation are microheterogeneous systems with contributions to microheterogeneity from both the heterogeneity of the individual polymers and the thermodynamic incompatibility of the components. © 2001 Elsevier Science B.V. All rights reserved.

Keywords: Thermoplastic interpenetrating polymer networks; Polyurethane; Styrene/acrylic acid copolymer; Microheterogeneity

1. Introduction

Interpenetrating polymer networks (IPNs) provide the possibility of effectively producing advanced multicomponent polymeric systems with new property profiles [1–3]. In IPNs at least one component is synthesized and/or crosslinked in the immediate presence of the other. In contrast to that, in thermoplastic IPNs (t-IPNs) the components are crosslinked by means of physical, instead of chemical, bonds. t-IPNs are intermediate between mixtures of linear polymers and IPNs; they behave like chemically crosslinked polymers at relatively low temperatures and as thermoplastics at high temperatures.

Segmented polyurethanes have been widely used as a component in IPNs [4–8]. Their versatile properties are generally attributed to their microphase-separated morphology, consisting of microdomains rich in hard segments (HS microdomains) and a microphase rich in soft segments (SS microphase) and arising from the thermodynamic incompatibility of HS and SS [9]. A variety of morphologies (homogeneous, phase-separated, co-continuous) has been observed in polyurethane IPNs, determined by the degree of compati-

* Corresponding author. Tel.: +30-1-772-2986; fax: +30-1-772-2932.
E-mail address: ppissis@central.ntua.gr.

PII: S0040-6031(01)00420-8

bility with the second component, the composition and the preparation conditions [4–8].

We report here, the results of detailed investigations of the structure–property relationships in mechanically blended t-IPNs of a crystallizable polyurethane (CPU) and a styrene/acrylic acid copolymer (S/AA). Several compositions of the t-IPNs were prepared by melting and pressing, and investigated by the combination of various thermal techniques: differential scanning calorimetry (DSC), thermomechanical analysis (TMA), thermally stimulated depolarization currents (TSDC) and thermally stimulated conductivity (TSC) measurements, as well as broadband dielectric relaxation spectroscopy (DRS). In a previous paper, t-IPNs prepared from a common solvent have been investigated [10].

2. Experimental

Details of the preparation of the individual CPU and S/AA (molar ratio 72/28) components have been given in [10]. CPU is physically crosslinked by means of strong bonds (hydrogen bonds and microcrystallites acting as effective crosslinking sites). S/AA may be considered as a linear thermoplastic polymer (acid form), although, significant physical crosslinking is expected to occur by means of hydrogen bonding. Sheets of the t-IPNs of different compositions were prepared from melting at 170°C and 6 MPa for 5–10 min.

TMA in tensile test mode, DRS and TSDC techniques and the equipment used have been described in [10]. For DSC, a Perkin-Elmer DSC 2 calorimeter was used from −120 to 180°C at a heating rate of 20°C/min. For TMA in bending mode, a polymer laboratories apparatus (Model PL-MK II) was used in the frequency range 0.1–100 Hz from −100 to 200°C. For TSC, a homemade equipment was used from 20 to 200°C [11].

3. Results and discussion

DSC measurements allowed the study of the glass transitions of CPU and S/AA in the t-IPNs at about −40 and 130°C, respectively, and the melting of butylene adipate glycol (BAG), the SS of CPU, at about 50°C. Table 1 lists the results of DSC measurements. Prior to the second heating run, the sample was quenched from 180 to below −120°C. t_{g1} in Table 1 is practically independent of composition in the range studied. It is lower for the quenched samples due to partial removal of constraints on the mobility of the amorphous part of CPU imposed by the BAG crystallites.

The DSC curve in the region of the glass transition of S/AA is complex already for the individual S/AA

Table 1
DSC experimental results[a]

Composition (% CPU)	t_{g1} (°C)		t_{g2} (°C)		t_m (°C)	
	Initial	Quenched	Initial	Quenched	Initial	Quenched
0	–	–	114	126	–	–
3	–	–	121	129	51	–
5	–	–	113	125	51	–
10	–	–	117	127	48	–
20	–	–	121	131	53	–
35	–	–	128	133	52	47
50	–	−38	128	133	50	46
80	−33	−38	129	134	50	47
90	−34	−37	–	–	54	50
95	−33	−37	–	–	55	48
97	−33	−37	–	–	56	47
100	−34	−39	–	–	55	47

[a] t_{g1} and t_{g2} are the glass transition temperatures of the CPU and S/AA components, respectively, and t_m is the melting temperature of BAG crystallites.

component. This is due to microphase separation into S and AA in the copolymer, arising from the formation of hydrogen bonding in the AA component [12]. As a result of that, two glass transitions contribute to the DSC curve in the region 120–140°C, the main one at higher temperatures due to the S component and the smaller one at lower temperatures due to the AA component (the molar ratio of S/AA being 72/28). The microphase separation into S and AA improves upon quenching, so that, t_{g2} in Table 1 (determined mostly by the S component) increases. t_{g2} in Table 1, in general, increases with increasing CPU content, in particular, at low CPU contents. This is explained in terms of physical interactions of COOH groups of AA and S/AA with the ester groups of the flexible CPU blocks, which results in a better microphase separation of AA and S in the S/AA component. Thus, hydrogen bonding between AA and CPU promotes microphase separation of both the CPU and the S/AA component.

For the initial samples, melting of CPU is already observed at 3% of CPU content, this result suggests that the two components retain their individual characteristics [6]. The lowering of t_m upon quenching is explained by lower sizes of the crystallites.

The mechanical spectra of CPU in Fig. 1 show the α relaxation due to the glass transition at about −15°C and a further relaxation, attributed to the crystalline phase at about 25°C. Melting is observed at about 50°C, in agreement with DSC (Table 1). The mechanical spectra of S/AA show α relaxation at 145°C and a shoulder in the region from 135 to 140°C. In agreement with the DSC results, the peak at 145°C is attributed to the glass transition of the S component of S/AA and the shoulder at 135–140°C to the glass transition of the AA component of S/AA. Thus, the initial S/AA is considered as a system with limited heterogeneity. Recent experiments have shown the increase of shoulder height with the increase of AA content in S/AA [12].

The viscoelastic properties of the t-IPNs with content of CPU more than 50% (Fig. 1; curves 4 and 5) are defined by S/AA. The results show that the t-IPNs under investigation are multiphase systems [6] and their viscoelastic properties depend strongly on the interpenetration of components and physical interactions between CPU and S/AA. The mechanical spectra show that t_g of both CPU and S/AA changes as the composition of the t-IPNs is changed; t_g of S/AA

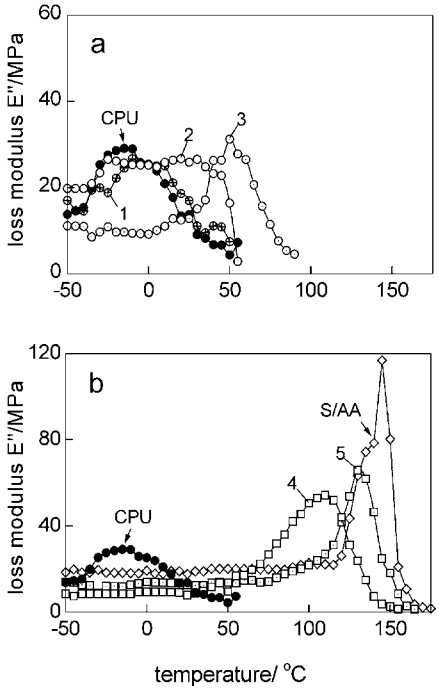

Fig. 1. Loss modulus E'' vs. temperature t from TMA measurements in tensile mode for t-IPNs of the following CPU/(S/AA) compositions: (a) 100/0 (CPU); 90/10 (1); 80/20 (2); 50/50 (3); (b) 100/0 (CPU); 20/80 (4); 10/90 (5); 0/100 (S/AA).

decreases by incorporation of 10 and 20% CPU. A possible explanation is that the viscoelastic behavior for these compositions and the temperature range of interest here is dominated by the AA component, as a result of microsegregation of AA due to formation of H-bonds between COOH-groups of AA and ester groups of flexible CPU blocks. The mechanical spectra are less conclusive with respect to variation of t_g of CPU upon addition of S/AA, where DSC shows no changes upon addition of 3, 5, 10 and 20% S/AA. The DSC results will be confirmed by TSDC.

The results of TMA measurements in bending mode, performed at 0.1, 1, 10 and 100 Hz, were in many aspects similar to those of TMA measurements in tensile mode. However, some characteristic differences were observed. As an example, Fig. 2 shows results obtained with t-IPN with 80% CPU. The temperature dependence of tan δ is similar to that of E'' in the tensile mode experiments (Fig. 1; curve 2), with significant losses at temperatures higher than about −30°C. These are due to the glass transition of

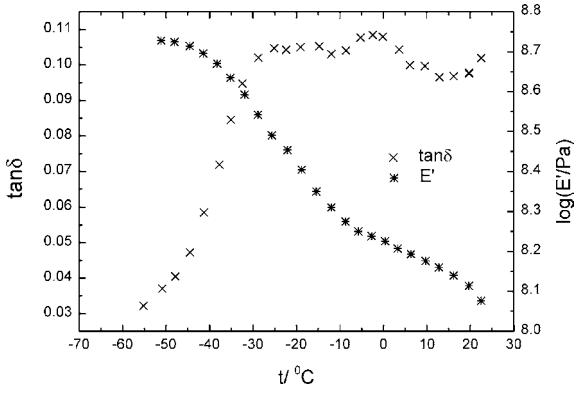

Fig. 2. Storage modulus (E', *) and loss tangent (tan δ, x) from TMA measurements in bending mode at 0.1 Hz for the t-IPN with 80% CPU.

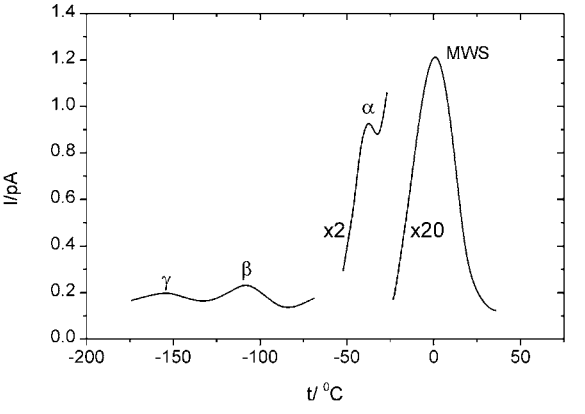

Fig. 3. TSDC plot for the t-IPN with 80% CPU.

the amorphous phase of CPU at lower temperatures (α) and of the crystalline phase of CPU at higher temperatures (α_c). The α relaxation is observed at about -15 to -20°C at 100 Hz, independent of composition for t-IPNs with up to 20% S/AA, in agreement with DSC and TMA tensile mode experiments. Its shift to lower temperatures with decreasing frequency of measurements will be discussed later in terms of the Arrhenius diagram. Additional relaxations, with respect to those of the individual components, indicative of mixed microphases and interfacial layers as a result of partial miscibility, contribute to the mechanical spectra in Figs. 1 and 2. It has been pointed out that additional relaxations may appear in IPNs due to different types of local regions of mobility [4].

Fig. 3 shows a typical TSDC plot for the sample with 80% CPU. TSDC allows for a fast characterization of the overall dielectric behavior (i.e. of molecular mobility) of the sample under investigation. The plot in Fig. 3 corresponds to measuring dielectric losses vs. temperature at low equivalent frequencies of 10^{-2}–10^{-4} Hz [10,11]. Four peaks are observed at -105, -110, -38 and 1°C. They are designated as γ, β, α and MWS (Maxwell–Wagner–Sillars) in the order of increasing temperature and assigned to CPU. γ and β are due to local relaxations [5,10], α is due to the glass transition and MWS is due to interfacial polarization [10]. The temperature position of the α peak, t_α, can be considered as a good measure of the calorimetric glass transition temperature [10]. Interestingly, t_α does not practically change with composition in the range 100–50% CPU (-32°C for 100 and 90% CPU, -36°C for 80% CPU and -35°C for 50% CPU), in agreement with DSC results. This behavior is less clear in the TMA results. We may conclude that the techniques used for detecting molecular mobility (DSC, TMA, TSDC, DRS) probe, in general, different spatial scales of local heterogeneity — a point to be taken into account in comparing with each others results obtained by different techniques. The peak temperature of the MWS peak was found to shift slightly to higher temperatures on addition of S/AA. Similar results in other polyurethane systems [13] have been shown to correlate with improved microphase separation into HS microdomains and SS microphase. The promotion of microphase separation of CPU in the t-IPNs is here attributed to strong physical interactions between the functional groups of CPU and AA.

Fig. 4 shows TSDC results at high temperatures. They demonstrate the melting of CPU in the pure CPU sample, observed also in the CPU-rich samples, the complexity of the behavior of the sample with 35% CPU, observed also in the mechanical spectra (Figs. 1 and 2), and the possibility to study the glass transition of S/AA in the S/AA-rich compositions (TSDC α peak for the sample with 10% CPU at about 120°C, is in good agreement with DSC results).

Results of DRS measurements are shown in Figs. 5–7 in isochronal (constant frequency) plots vs. temperature, to stress the similarities with the other thermal techniques employed in this work. They have

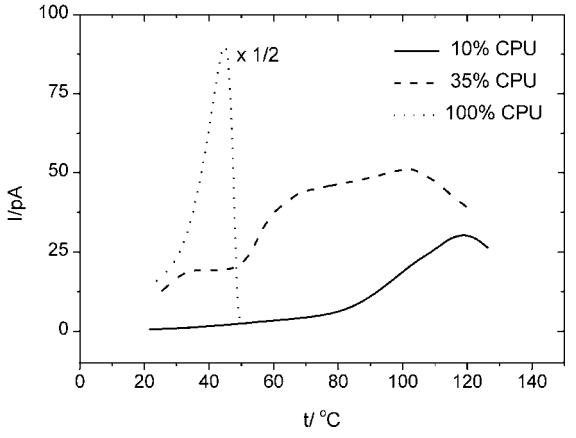

Fig. 4. High temperature TSDC plots for samples indicated on the plot.

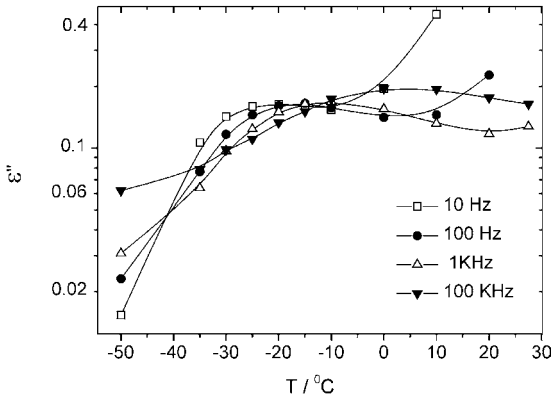

Fig. 6. Imaginary part of dielectric permittivity ε'' vs. temperature for CPU at several frequencies indicated on the plot. The lines are guides for the eye.

been replotted from data obtained in isothermal DRS scans. The comparative isothermal DRS plots (not shown here) allow to classify the t-IPNs into two groups, those with 50% and more CPU and those with less than 50% CPU, in agreement with the mechanical data in Fig. 1. In the first group CPU is the continuous phase, whereas in the second group CPU is dispersed in the S/AA matrix [7,8]. Figs. 5 and 6 show plots of the real and imaginary part of dielectric permittivity, ε' and ε'', respectively, for the individual CPU component in the temperature region of the glass transition. Similar to TMA, the α relaxation is observed as a step in $\varepsilon'(t)$ and as a peak in $\varepsilon''(t)$, both shifting to higher temperatures with increasing frequency of measurements. Bearing this shift in mind, the results correlate well with those of DSC, TMA and TSDC. At low frequencies and high temperatures, conductivity effects dominate in the $\varepsilon''(t)$ plot.

Fig. 7 shows $\varepsilon''(t)$ for the t-IPN with 3% CPU at several fixed frequencies in the temperature region of the glass transition of the S/AA component. The α relaxation, located at about 140°C at 1 kHz, in rather good agreement with the TMA results (Fig. 1) and DSC results (Table 1), shifts to higher temperatures with increasing frequency of observation. DC conductivity at these high temperatures increases rapidly

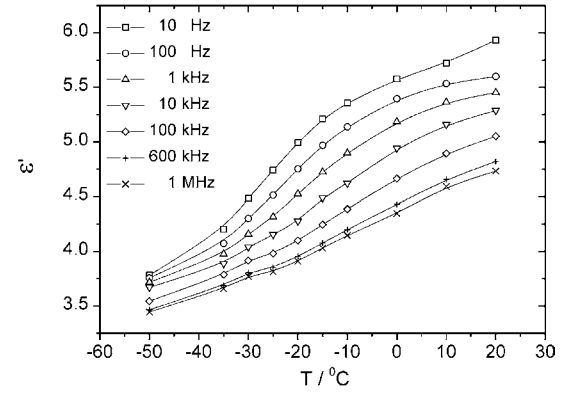

Fig. 5. Real part of dielectric permittivity ε' vs. temperature for CPU at several frequencies indicated on the plot. The lines are guides for the eye.

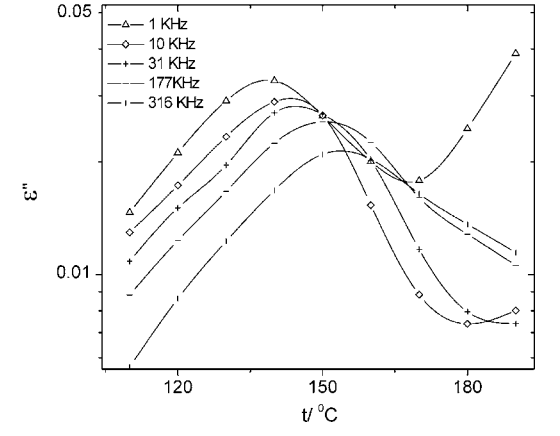

Fig. 7. Imaginary part of dielectric permittivity ε'' vs. temperature for the t-IPN with 3% CPU at several frequencies indicated on the plot. The lines are guides for the eye.

with increasing CPU content of the t-IPNs, so that conductivity effects dominate over the whole frequency range of measurements for CPU contents larger than about 5%. Therefore, the dependence of the frequency or temperature position of the α relaxation of the S/AA component of CPU content could not be studied in wide ranges, as it was done for t_g in DSC (Table 1), the results for the compositions studied being consistent with those of the DSC measurements.

Fig. 8 shows the Arrhenius plot for the α relaxation associated with the glass transition of the CPU component for the samples with 80 and 100% CPU on the basis of the DRS and the TMA results, with TSDC and DSC data being also included (TMA data for 97 instead of 100% CPU). The DSC points in Fig. 8 correspond to the t_g values of −33 and −34°C (first heating run, to have similar experimental conditions with the other techniques) for the t-IPNs with 80 and 100% CPU, respectively, and the equivalent frequency f_{equiv} of 20 mHz. f_{equiv} has been obtained from the equation [14]

$$f_{equiv} = \frac{b}{2\pi\alpha\delta T} \quad (1)$$

where b is the cooling rate (20°C/min, equal to the heating rate), α a constant of the order 1 and δT the mean temperature fluctuation (of the order 2°C/min) [15]. The TSDC points in Fig. 8 correspond to the TSDC peak temperature t_α of −32 and −36°C for t-IPNs with 80 and 100% CPU, respectively, and the equivalent frequency f_{equiv} of 1.6 mHz, corresponding to α relaxation time of 100 s [10,13], f_{equiv} is defined as the frequency of DRS measurements which give a maximum in ε'' at the temperature t_α.

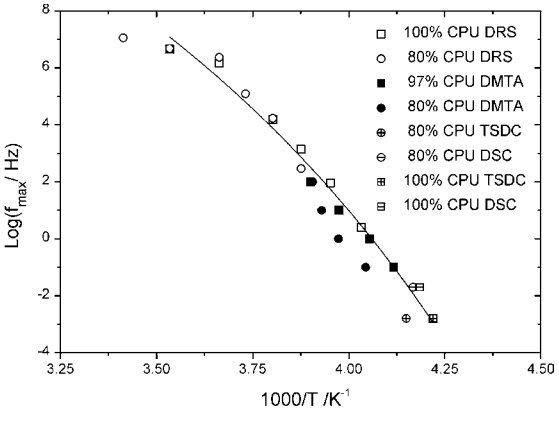

Fig. 8. Arrhenius plot for the α relaxation of the CPU component with data obtained by the techniques and for the samples indicated on the plot. The line is a VTF fit to the data for the sample with 100% CPU (97% CPU for TMA).

The TMA and DRS results in Fig. 8 agree well with each other, bearing in mind that the former refer to a modulus (modulus, E) and tan δ and the latter to a compliance (dielectric permittivity, ε) and ε''. The equivalent frequencies of DSC and TSDC, out of the frequency range of DRS and TMA, compare rather well with TMA and DRS. As for the comparison between the two t-IPNs in Fig. 8, the DRS data show no difference, in agreement with DSC. The TSDC and TMA data, on the other hand, suggest that the α process becomes slower on addition of S/AA.

The line in Fig. 8 is a fit of the Vogel–Tammann–Fulcher (VTF) equation [14]

$$f_{max} = A \exp\left(-\frac{B}{T - T_0}\right) \quad (2)$$

with empirical temperature-independent parameters A, B and T_0, to the experimental data for the CPU individual component (the t-IPN with 97% CPU for TMA) considering all the techniques employed. The fit is good with reasonable values for the parameters, $\log A = 22.8$, $B = 4290$ K, $T_0 = 165$ K.

4. Conclusions

The t-IPNs under investigation can be classified into two groups with high and low contents of CPU showing essentially the behavior of CPU and of S/AA, respectively. However, deviations from additivity for several properties indicate interactions between the two components, caused by the formation of H-bonds between their functional groups. H-bonding results in partial miscibility between the two components. Microphase separation and partial miscibility is reflected in different ways by using various techniques, due to different length-scales of microheterogeneity probed by the various techniques.

Acknowledgements

Work supported by INTAS 97-1936 and by the Greek–Romanian bilateral exchange programme.

References

[1] L.H. Sperling, Interpenetrating Polymer Networks and Related Materials, Plenum Press, New York, 1981.
[2] D. Klempner, L.H. Sperling, in: L.A. Utracki (Ed.), Interpenetrating Polymer Networks, Advanced Chemistry Series No 239, American Chemistry Society, Washington, DC, 1994.
[3] D. Klempner, in: K.C. Frisch (Ed.), Advances in Interpenetrating Polymer Networks, Vol. IV, Technomic Publishing Co., Lancaster, PA, 1994.
[4] C. Mai, G.P. Johari, J. Polym. Sci., Polym. Phys. Ed. 25 (1987) 1903.
[5] S.B. Pandit, V.M. Nadkarni, Macromolecules 27 (1994) 4583, 4595.
[6] W.-Y. Chiang, D.-M. Chang, J. Mater. Sci. 32 (1997) 4985.
[7] S. Dadbin, R.P. Burford, R.P. Chaplin, Polymer 37 (1996) 785.
[8] S. Bai, D.V. Khakhar, V.M. Nadkarni, Polymer 38 (1997) 4319.
[9] J.T. Koberstein, A.F. Galambos, L.M. Leung, Macromolecules 25 (1992) 6195.
[10] A. Kyritsis, P. Pissis, O.P. Grigorieva, L.M. Sergeeva, A.A. Brovko, O.N. Zimich, E.G. Privalko, V.I. Shtompel, V.P. Privalko, J. Appl. Polym. Sci. 73 (1999) 385.
[11] E.R. Neagu, R.M. Neagu, Phys. Stat. Sol. A 144 (1994) 429.
[12] L.M. Sergeeva, O.N. Zimich, O.P. Grigorieva, A.A. Brovko, N.S. Nedashkovskaya, Polym. Int., in press.
[13] P. Pissis, A. Kanapitsas, Yu.V. Savelyev, E.R. Akhranovich, E.G. Privalko, V.P. Privalko, Polymer 39 (1998) 3431.
[14] E. Donth, Relaxation and thermodynamics in polymers, Glass Transition, Akademie, Berlin, 1992.
[15] A. Hensel, J. Dobbertin, J.E.K. Schawe, A. Boller, C. Schick, J. Therm. Anal. 46 (1996) 935.